

The Synthesis of Copper(II) Salicylaldiminato Complexes and their Catalytic Activity in the Hydroxylation of Phenol

Juanita L. van Wyk^a, Selwyn Mapolie^a, Anders Lennartson^b, Mikael Håkansson^b, and Susan Jagner^c

^a Chemistry Department, University of the Western Cape, Private Bag X17, Bellville, 7535, South Africa

^b Department of Chemistry, Göteborg University, SE-412 96 Göteborg, Sweden

^c Department of Chemical and Biological Engineering, Chalmers University of Technology, SE-412 96 Göteborg, Sweden

Reprint requests to S. Mapolie. E-mail: smapolie@uwc.ac.za

Z. Naturforsch. **2007**, 62b, 331–338; received November 13, 2006

Dedicated to Prof. Helgard G. Raubenheimer on the occasion of his 65th birthday

The synthesis of copper(II) salicylaldiminato complexes and their application in the catalytic hydroxylation of phenol is reported. Tetracoordinated copper complexes ($\text{Cu}(\text{L}^n)_2$) were obtained by reacting the *N*-phenylsalicylaldimine ligands ($\text{HL}^1 - \text{HL}^7$) with copper acetate in a 2 : 1 mole ratio. The reaction of *N*-(2,6-diisopropyl)phenyl-3,5-di-*tert*-butylsalicylaldimine (HL^7) with copper acetate in a 1 : 1 mole ratio afforded a dinuclear complex, which was not obtained with the other ligand systems. All complexes were characterized using FT-IR and elemental analysis. X-Ray crystal structures of complexes **2**, **5** and **8** have also been obtained. The catalytic activity of these complexes was evaluated in the hydroxylation of phenol using oxygen and hydrogen peroxide as co-oxidants in aqueous media in the pH range 3–6. All complexes studied were found to be active for the hydroxylation process over the pH range studied with higher selectivity for catechol formation.

Key words: Salicylaldimine, Tetracoordinated Copper(II) Complexes, Hydroxylation, Phenol

Introduction

Due to environmental concerns there has been an increase in the demand by industry to introduce processes which are environmentally and economically sustainable. As a result much attention has been focused on developing catalytic processes, which utilize cheap, abundant and non-toxic oxidants such as dioxygen and hydrogen peroxide. Over the past decade there has been an increase in the interest in transition metal complexes based on porphyrins, phthalocyanines and Schiff bases. These complexes are widely used as peroxidase mimics [1–3] and have been employed to study the oxidation of phenol using hydrogen peroxide as oxidant. Currently the oxidation of phenol with hydrogen peroxide is of significance since the process provides an environmentally friendly means of obtaining the dihydroxybenzenes, hydroquinone (HQ) and catechol (CT), which are widely used as raw materials in the agrochemical and fine chemical industries. There are a number of industrial processes for the production of these dihydroxybenzenes, however the

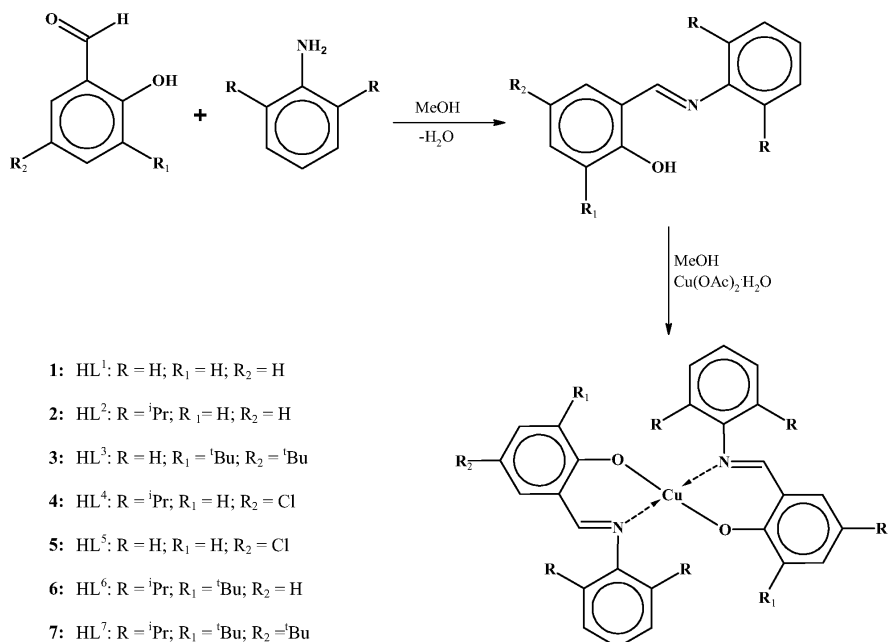
catalytic systems employed are environmentally hazardous. Poor selectivities are also obtained and a significant amount of tar material is often produced. Recently catalysts based on zeolites [4, 5] have been developed to improve the selectivities and the economical viability of this process. Although a commercial process has been developed employing these zeolite catalytic systems [6], the utilization of these catalysts industrially has been limited by their complicated synthetic route and the associated high cost. In this paper the synthesis of copper(II) salicylaldiminato complexes **1–8** is described and the catalytic activity of these complexes evaluated in the hydroxylation of phenol to HQ and CT using oxygen and hydrogen peroxide as co-oxidants in aqueous media.

Results and Discussion

All Schiff base ligands were synthesized according to a well-established synthetic procedure which involved the condensation of a substituted salicylaldehyde with the appropriate aromatic amine [7]. Ligands

Table 1. Characterization data for mono-functional salicylaldimine ligands HL¹ – HL⁷.

Ligand	NMR spectra (ppm) ^a	Anal. found (calcd.)	IR spectra (cm ⁻¹) ^b
HL¹ (R = H; R ₁ = H; R ₂ = H), m. p. 49–50 °C	¹ H NMR: δ = 1.25 (d, 12H), 3.07 (sept, 2H), 6.9–7.15 (m, 2H), 7.4–7.46 (m, 2H), 8.38 (s, 1H) ¹³ C NMR: δ = 23.48, 28.11, 117.32, 118.68, 118.98, 123.23, 125.43, 132.17, 133.19, 138.66, 146.19, 161.23, 166.57	C ₁₃ H ₁₁ NO: C 78.79 (79.16), H 5.58 (5.62), N 7.74 (7.10)	ν(C=N) 1617 ν(C–O) 1273
HL² (R = <i>i</i> Pr; R ₁ = H; R ₂ = H), m. p. 55–57 °C	¹ H NMR: δ = 1.25 (d, 12H), 3.07 (sept, 2H), 6.9–7.15 (m, 2H), 7.4–7.46 (m, 2H), 8.38 (s, 1H) ¹³ C NMR: δ = 23.48, 28.11, 117.32, 118.68, 118.98, 123.23, 125.43, 132.17, 133.19, 138.66, 146.19, 161.23, 166.57	C ₁₉ H ₂₃ NO: C 81.24 (81.10), H 8.70 (8.24), N 5.22 (4.98)	ν(C=N) 1625 ν(C–O) 1279
HL³ (R = H; R ₁ = <i>t</i> Bu; R ₂ = <i>t</i> Bu), m. p. 108–110 °C	¹ H NMR: δ = 1.29 (s, 9H), 1.45 (s, 9H), 6.9–7.2 (m, 4H), 7.4 (m, 3H), 8.60 (s, 1H), 13.69 (s, 1H) ¹³ C NMR: δ = 29.46, 31.49, 34.19, 35.13, 118.34, 121.16, 126.50, 126.8, 127.99, 129.32, 137.02, 140.57, 148.79, 158.28, 163.81	C ₂₁ H ₂₇ NO: C 81.50 (81.51), H 8.69 (7.89), N 4.15 (4.53)	ν(C=N) 1613 ν(C–O) 1272
HL⁴ (R = <i>i</i> Pr; R ₁ = H; R ₂ = Cl), m. p. 114–115 °C	¹ H NMR: δ = 1.24 (d, 12H), 3.02 (sept, 2H), 7.05 (d, 1H), 7.3 (s, 3H), 7.4 (s, 2H), 8.31 (s, 1H) ¹³ C NMR: δ = 23.51, 28.19, 118.96, 119.40, 123.35, 123.73, 125.77, 131.23, 133.05, 138.59, 145.77, 159.82, 165.48	C ₁₉ H ₂₂ ClNO: C 72.19 (72.25), H 6.98 (7.02), N 4.02 (4.48)	ν(C=N) 1625 ν(C–O) 1273
HL⁵ (R = H; R ₁ = H; R ₂ = Cl), m. p. 107–108 °C	¹ H NMR: δ = 6.92 (m, 1H), 7.2–7.4 (m, 7H), 8.51 (s, 1H), 13.26 (br s, 1H) ¹³ C NMR: δ = 118.84, 119.97, 123.66, 127.32, 129.48, 131.20, 132.89, 148.01, 159.72, 161.26	C ₁₃ H ₁₀ ClNO: C 67.32 (67.40), H 4.26 (4.35), N 5.60 (6.05)	ν(C=N) 1614 ν(C–O) 1276
HL⁶ (R = <i>i</i> Pr; R ₁ = <i>t</i> Bu; R ₂ = H), m. p. (66–68 °C	¹ H NMR: δ = 1.26 (d, 12H), 1.57 (s 9H), 3.07 (sept, 2H), 6.89 (t, 1H), 7.26 (s, 3H), 7.6 (dd, 2H), 8.37 (s, 1H) ¹³ C NMR: δ = 23.60, 28.14, 29.46, 34.99, 118.21, 118.58, 123.25, 125.36, 130.4, 130.58, 137.86, 138.91, 146.35, 160.72, 167.28	C ₂₃ H ₃₁ NO: C 81.43 (81.85), H 9.24 (9.26), N 3.95 (4.15)	ν(C=N) 1618 ν(C–O) 1269
HL⁷ (R = <i>i</i> Pr; R ₁ = <i>t</i> Bu; R ₂ = <i>t</i> Bu), m. p. 79–81 °C	¹ H NMR: δ = 1.26 (d, 12H), 1.42 (s 9H), 1.58 (s 9H), 3.11 (sept, 2H), 7.24 (m, 4H), 7.59 (d, 1H), 8.38 (s, 1H) ¹³ C NMR: δ = 23.62, 28.06, 29.52, 31.49, 34.21, 35.2, 117.77, 123.17, 125.23, 126.65, 128.10, 137.18, 138.88, 140.48, 146.43, 158.46, 167.53	C ₂₇ H ₃₉ NO: C 82.52 (82.39), H 10.13 (9.99), N 3.92 (3.56)	ν(C=N) 1620 ν(C–O) 1270

^a Recorded in CDCl₃; ^b recorded as nujol mulls between NaCl plates.Scheme 1. Synthesis of salicylaldimine ligands HLⁿ and copper(II) complexes 1–7.

Complex	Formula	Anal found (calcd.)			IR spectra (cm ⁻¹) ^a	
		C	H	N	$\nu(\text{C}=\text{N})$	$\nu(\text{C}-\text{O})$
1	C ₂₆ H ₂₀ CuN ₂ O ₂ · 1/2H ₂ O	67.85 (67.17)	4.17 (4.42)	6.01 (6.14)	1606	1327
2	C ₃₈ H ₄₄ CuN ₂ O ₂	72.90 (73.11)	7.11 (7.10)	4.45 (4.49)	1602	1323
3	C ₄₂ H ₅₂ CuN ₂ O ₂	74.57 (74.14)	7.73 (7.70)	4.13 (4.12)	1609	1317
4	C ₃₈ H ₄₂ Cl ₂ CuN ₂ O ₂	65.46 (65.84)	6.12 (6.11)	3.77 (4.04)	1610	1322
5	C ₂₆ H ₁₈ Cl ₂ CuN ₂ O ₂ · 1/2H ₂ O	58.41 (58.49)	3.23 (3.46)	5.54 (5.34)	1606	1322
6	C ₄₆ H ₆₀ CuN ₂ O ₂	74.81 (75.01)	8.17 (8.21)	3.78 (3.80)	1602	1318
7	C ₅₄ H ₇₆ CuN ₂ O ₂ · 2H ₂ O	73.62 (73.32)	8.73 (9.06)	2.53 (2.97)	1610	1324
8	C ₅₆ H ₈₀ Cu ₂ N ₂ O ₅ · H ₂ O	66.50 (66.84)	8.13 (8.21)	2.75 (2.78)	1614	1325

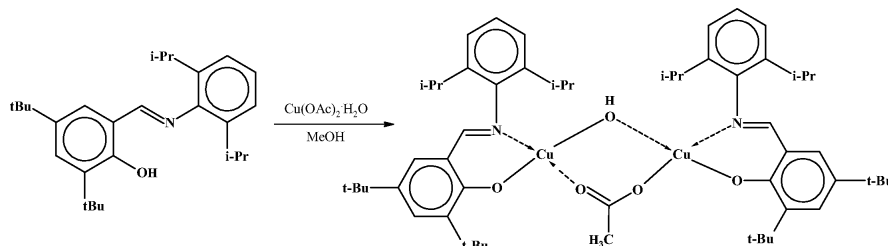
Table 2. Characterization data for copper(II) salicylaldiminato complexes **1–8**.^a Recorded as nujol mulls between NaCl plates.

Compound	2	5	8
Empirical formula	C ₃₈ H ₄₄ CuN ₂ O ₂	C ₂₆ H ₁₈ Cl ₂ CuN ₂ O ₂	C ₅₆ H ₈₀ Cu ₂ N ₂ O ₅
<i>Mr</i>	624.3	524.9	988.3
Crystal system	triclinic	monoclinic	monoclinic
Space group	<i>P</i> $\bar{1}$	<i>C</i> 2/ <i>c</i>	<i>P</i> 2 ₁ / <i>c</i>
<i>a</i> , Å	8.0725(16)	23.634(7)	14.944(2)
<i>b</i> , Å	10.2332(9)	9.337(2)	24.968(3)
<i>c</i> , Å	11.7022(3)	15.087(5)	14.736(2)
α , deg.	60.62(2)	90	90
β , deg.	76.39(3)	137.343(7)	94.539(4)
γ , deg.	81.64(4)	90	90
<i>V</i> , Å ³	818.2(1)	2256(1)	5481(1)
<i>Z</i>	1	4	4
<i>F</i> (000), e	331	1068	2112
<i>D</i> calc, g cm ⁻³	1.27	1.54	1.20
μ (MoK α), cm ⁻¹	7.0	12.32	8.21
Temperature, °C	20(2)	20(2)	20(2)
2θ range, deg.	4.0 < 2θ < 54.0	7.6 < 2θ < 54.0	3.6 < 2θ < 52.0
Absorption correction	empirical	empirical	empirical
Data / refined parameters	3230 / 206	2235 / 151	9953 / 589
<i>R</i> ₁ [<i>I</i> ≥ 2σ(<i>I</i>)]	0.055	0.032	0.064
<i>wR</i> ₂ (all reflections)	0.119	0.091	0.167
Max/min residual electr. density, e Å ⁻³	0.45 / -0.86	0.27 / -0.35	1.33 / -0.40

Table 3. Crystallographic data for **2**, **5** and **8**.

$$R_1 = \frac{\sum \|F_o\| - |F_c|}{\sum \|F_o\|};$$

$$wR_2 = \left\{ \frac{\sum [w(F_o^2 - F_c^2)^2]}{\sum [w(F_o^2)^2]} \right\}^{1/2}.$$

Scheme 2. Synthesis of the dinuclear complex **8**.

were obtained as pale yellow to orange yellow solids in good yields. Structural data for the ligand systems HL¹–HL⁷ and copper complexes **1–8** are provided in Tables 1 and 2, respectively. The mononuclear tetracoordinated copper(II) complexes **1–7** were quite readily obtained *via* a 2 : 1 mole equivalent reaction of the appropriate ligand with copper acetate. The reaction of HL⁷ in a 1 : 1 mole ratio with copper acetate afforded the dinuclear complex **8**. Similar bimetallic species were not obtained with the other ligand systems. The formation of bimetallic species has been reported in the cases where bi- and tridentate salicylaldimine ligands were reacted with metal halides, nitrates and perchlo-

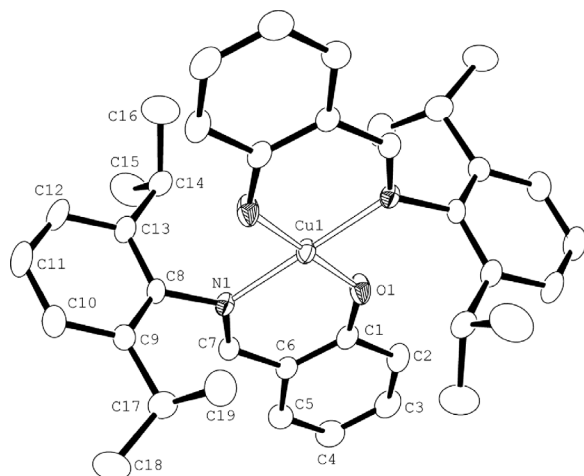
rates [8]. Alkoxy bridged dimers containing iron [9] and zinc [10] have also been reported recently.

IR Spectra

A broad band is observed in the range 2800–3000 cm⁻¹ in the IR spectra of the free ligands under investigation. This band is attributed to the O–H stretching vibration. The occurrence of the band at such a low wavenumber is characteristic of these ligands and is an indication of fairly extensive hydrogen bonding [11]. The C=N band is observed in the region 1613–1625 cm⁻¹ for the free ligands, but is shifted

Table 4. Selected bond lengths (Å) and angles (deg) for the core of **2**.

Cu(1)–N(1)	1.999(2)	O(1)–Cu(1)–N(1)	91.39(9)
Cu(1)–O(1)	1.869(2)	O(1)–Cu(1)–N(1) ⁱ	88.61(9)

Symmetry code: ⁱ $-x, -y, 1-z$.Fig. 1. The molecular structure of **2** and atomic numbering scheme adopted. Cu(1) is situated on a crystallographic centre of symmetry.

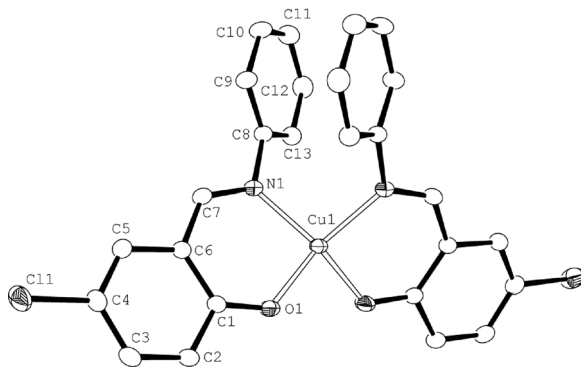
to 1602–1614 cm^{-1} in the spectra of the copper complexes, which indicates coordination of the azomethine nitrogen atom to the metal [12]. Coordination of the ligand to the metal is further confirmed by the shift in the phenoxy C–O stretching vibration from 1269–1279 cm^{-1} to a higher frequency upon M–O coordination.

X-Ray crystallography

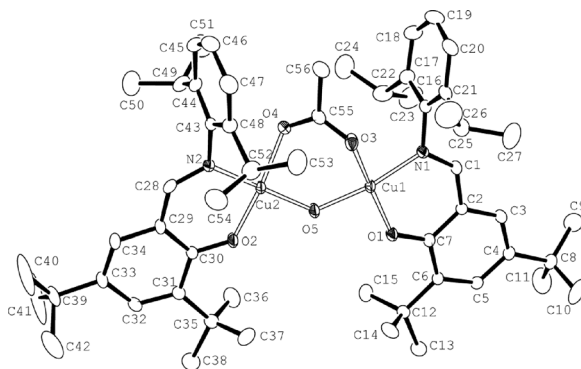
The crystal structures of complexes **2**, **5** and **8** are shown in Figs. 1–3, respectively. X-Ray crystallography revealed the Schiff base ligands to coordinate in a bidentate fashion with two ligands coordinating to one copper centre for both complexes **2** and **5**. However, the ligands of complex **2**, which contain *i*Pr substituents on the imino-bound aromatic ring, are coordinated in a *trans* arrangement whereas the ligands of complex **5**, which do not contain substituents on the imino-bound aromatic ring coordinate in a *cis* arrangement. Similar results have been obtained with cobalt analogues of this type of ligand systems [13]. The crystal structure of complex **8** revealed coordination of one ligand per copper centre with an acetoxy and a hydroxy group bridging between the two copper centres. Note: In **2**, Cu is situated on a centre of symmetry so that

Table 5. Selected bond lengths (Å) and angles (deg) for the core of **5**.

Cu(1)–N(1)	1.985(1)	O(1)–Cu(1)–N(1)	93.56(6)
Cu(1)–O(1)	1.901(1)	O(1)–Cu(1)–N(1) ⁱ	151.86(6)
		O(1)–Cu(1)–O(1) ⁱ	88.07(8)
		N(1)–Cu(1)–N(1) ⁱ	97.93(8)

Symmetry code: ⁱ $-x, y, 1.5-z$.Fig. 2. The molecular structure of **5** and atomic numbering scheme adopted. Cu(1) is situated on a crystallographic two-fold axis.Table 6. Selected bond lengths (Å) and angles (deg) for the core of **8**.

Cu(1)–N(1)	1.951(3)	Cu(2)–N(2)	1.952(3)
Cu(1)–O(1)	1.884(3)	Cu(2)–O(2)	1.881(3)
Cu(1)–O(3)	1.960(3)	Cu(2)–O(4)	1.956(4)
Cu(1)–O(5)	1.880(3)	Cu(2)–O(5)	1.880(3)
N(1)–Cu(1)–O(1)	93.6(1)	N(2)–Cu(2)–O(2)	93.1(1)
N(1)–Cu(1)–O(3)	91.9(1)	N(2)–Cu(2)–O(4)	88.1(1)
N(1)–Cu(1)–O(5)	166.5(1)	N(2)–Cu(2)–O(5)	166.8(1)
O(1)–Cu(1)–O(3)	166.4(1)	O(2)–Cu(2)–O(4)	165.8(1)
O(1)–Cu(1)–O(5)	89.6(1)	O(2)–Cu(2)–O(5)	90.1(1)
O(3)–Cu(1)–O(5)	91.9(1)	O(4)–Cu(2)–O(5)	92.0(1)

Fig. 3. The molecular structure of **8** and atomic numbering scheme adopted.

N(1)–Cu(1)–N(1)ⁱ and O(1)–Cu(1)–O(1)ⁱ are both exactly 180°. In **5**, Cu(1) is situated on a twofold axis. The phenyl rings attached to N(1) and N(1)ⁱ are almost co-planar [dihedral angle 6.3(1)°], the distance between the ring centroids being 3.62 Å, indicative of weak intramolecular $\pi \cdots \pi$ interactions. Crystal and experimental data are summarized in Tables 3–6.

Catalyst evaluation

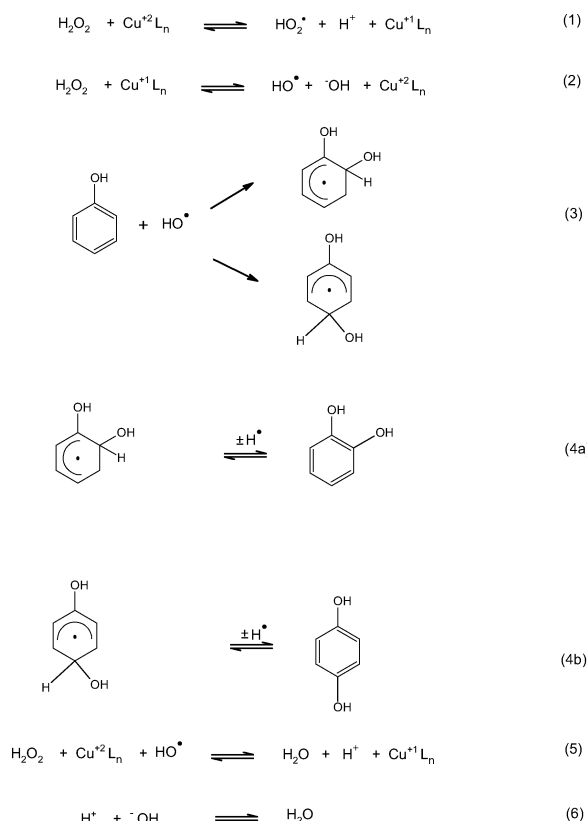
The hydroxylation of phenol catalyzed by complexes **1–4** and complex **8** was studied in deionized water in the pH range 3–6 using appropriately buffered solutions. All reactions were performed under an oxygen atmosphere using 6 % H₂O₂ as co-oxidant. A substrate to metal ratio of 100:1 and a 1:1 mole ratio of phenol to H₂O₂ was used for all reactions. Results for the hydroxylation reactions performed are shown in Table 7.

Catalyst activity

All the complexes evaluated were found to be active for phenol hydroxylation. The catalyst activity was tested over a range of pH values in order to evaluate to what extent the acidity of the medium affects phenol conversion. It was found that the complexes perform better at moderately acidic pH values. The highest phenol conversion (77 %) was obtained with complex **8** at pH 6. This however is only slightly higher than the conversion obtained for the other complexes at similar pH values. Reactions were also attempted in alkaline media, but these showed no phenol consumption. The results obtained are in agreement with what has been reported in the literature for other metal-mediated phenol hydroxylation processes [14]. The results can be explained in terms of the generally accepted reaction mechanism for the oxidation of aromatic hydrocarbons [15].

The accepted reaction pathway can basically be summarized by the steps outlined in Scheme 3.

Our results are in general agreement with what has been reported in the literature. Thus the effectiveness of the hydroxylation process in acidic media can be explained in terms of some of the steps outlined in Scheme 3. Acidic media enhance the metal-mediated decomposition of H₂O₂ to the hydroxyl radical, which is an important species in the hydroxylation of phenol [16–17]. The decomposition of the peroxide is shown in step 2 (Scheme 3). This step can clearly be enhanced in moderately acidic media by the removal



Scheme 3. Proposed reaction pathway for phenol hydroxylation.

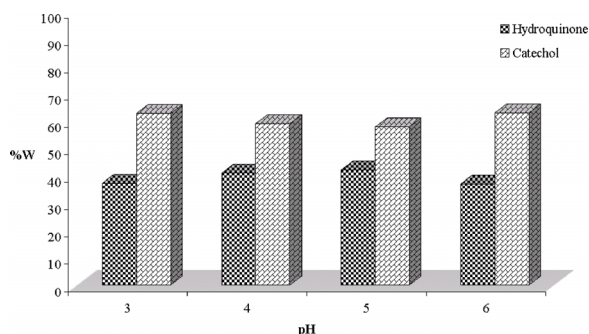
of OH[−] anions from the reaction mixture. Conversely, at alkaline pH, the high OH[−] concentration shifts the equilibrium in step 2 to the left, thus lowering the hydroxyl radical concentration. This is what we observe, as all the catalysts are inactive at pH values above pH 7. We however found that too low a pH also has a detrimental effect on catalyst activity. Thus the catalysts are ineffective at pH 2 and below, with no phenol hydroxylation being observed. At such low pH values we have the possibility of step 1 in Scheme 3 being retarded. This ultimately has a negative effect on the production of the hydroxyl ions (step 2). In several of our experiments we found that the optimum pH was around 5 or 6.

We also attempted to perform the reactions in acetonitrile as solvent. In this case no oxidation products were observed for the catalyst systems evaluated. A possible reason for this is that in acetonitrile the generation of the hydroxyl radical is retarded as a result of coordination of the solvent to the metal centre. This prevents H₂O₂ interaction with the active site and hin-

Table 7. Effect of pH on the catalytic activity of complexes **1–4** and **8**^a.

Catalyst	pH	%W		%PhOH Conversion	TOF ^c
		Dihydroxybenzenes ^b			
		HQ	CT		
1	3	37.18	62.82	56	9.4
	4	40.99	59.01	69	11.5
	5	42.01	57.99	72	12.0
	6	37.02	62.98	71	11.9
2	3	38.13	61.87	49	8.2
	4	31.99	68.01	73	12.2
	5	37.86	62.14	74	12.4
	6	32.69	67.31	65	10.8
3	3	32.67	67.33	62	10.4
	4	34.39	65.61	68	11.4
	5	36.53	63.47	62	10.3
	6	35.77	64.23	73	12.2
4	3	37.45	62.55	66	11.0
	4	28.74	71.26	66	11.0
	5	33.63	66.37	63	10.5
	6	30.40	69.60	72	12.0
8	3	31.79	68.21	65	10.9
	4	28.24	71.76	64	10.7
	5	32.32	67.68	73	12.1
	6	39.11	60.89	77	12.8

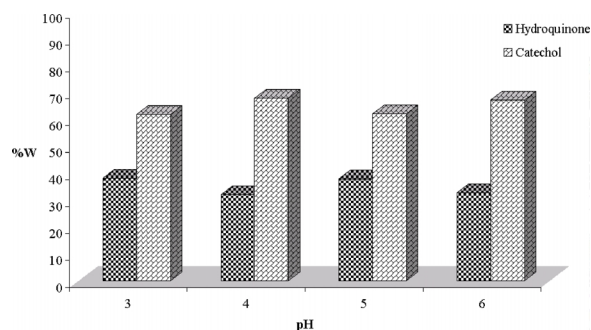
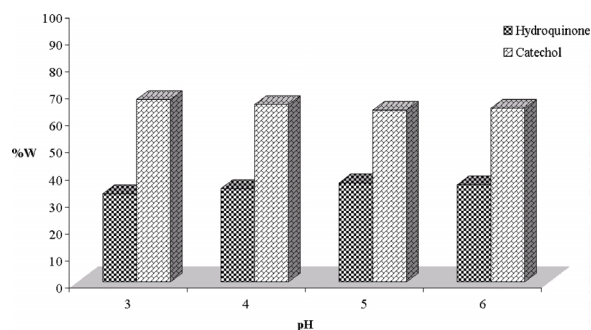
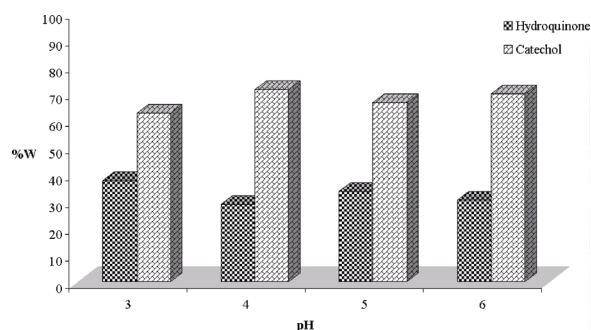
^a Reaction performed in 10 mL H₂O, Phenol : Cu = 100 : 1; 10 °C at 1 atm O₂; 6 % H₂O₂ as co-oxidant; Phenol : H₂O₂ = 1 : 1; ^b HQ = Hydroquinone; CT = Catechol; product distribution given on a tar free basis; ^c TOF = (mol phenol consumed/mol Cu)/hour.

Chart 1. Effect of pH on hydroquinone : catechol ratio for catalyst **1**.

ders the decomposition of hydrogen peroxide to the hydroxyl radical. Another potential problem could be the reaction of the organic solvent with any HO• radical, if it should form in the first place. Similar observations have previously been reported in the literature for processes in which organic solvents react with the active hydroxy radical [17].

Catalyst selectivity

The major products observed under the conditions described were hydroquinone (HQ) and catechol (CT).

Chart 2. Effect of pH on hydroquinone : catechol ratio for catalyst **2**.Chart 3. Effect of pH on hydroquinone : catechol ratio for catalyst **3**.Chart 4. Effect of pH on hydroquinone : catechol ratio for catalyst **4**.

In some instances minute traces of benzoquinones (BQ) were also detected. In almost all cases the catechol to hydroquinone ratio was around 2 : 1, with the exception of complex **1**, which produces slightly higher levels of hydroquinone than the other catalysts. In the latter case the CT : HQ ratios are around 1.5 : 1. The predominance of catechol over hydroquinone is not unexpected for copper-mediated hydroxylations occurring *via* the free radical process. It has previously been reported that the hydroxylation occurs *via* a pathway which involves initial weak coordination of both

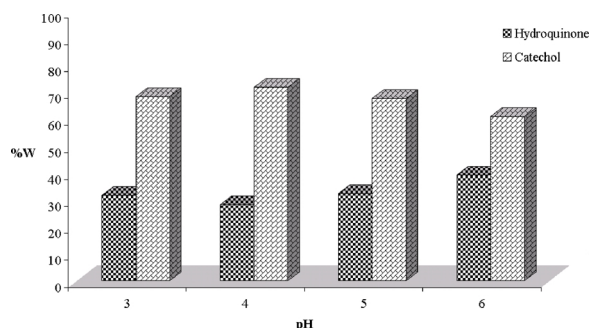


Chart 5. Effect of pH on hydroquinone : catechol ratio for catalyst **8**.

phenol and H_2O_2 to the active site. The anchoring of the two reaction partners in close proximity leads predominantly to a *cis* arrangement, which in turn results in *ortho*-substitution of the phenol [18].

Conclusions

Copper(II) complexes of *N*-phenylsalicylaldimine ligands were synthesized and the molecular structure of complexes **2**, **5** and **8** were determined using single crystal X-ray crystallography. The crystal structure of complex **8** revealed the formation of a dinuclear copper complex while both **2** and **5** are mononuclear complexes with coordination of the ligands *trans* and *cis*, respectively. The catalytic activity of complexes **1–4** and **8** were evaluated in the hydroxylation of phenol in aqueous media under pH-controlled conditions. For all catalysts the major products detected were HQ and CT although the catalyst appeared to be more selective towards the formation of CT. There was no significant pH effect in terms of catalyst activity and only a slight pH effect was observed favouring the formation of CT for all catalysts. For complexes containing substituents on the aromatic ring attached to the imino nitrogen atom, a slight steric effect was observed which favored the formation of CT.

Experimental Section

All chemicals were of reagent grade and used as received. All solvents were dried over the appropriate drying agent and distilled prior to use. Reactions and other manipulations were carried out using a dual vacuum/nitrogen line and standard Schlenk techniques unless stated otherwise. ^1H NMR (200 MHz) and ^{13}C NMR (50 MHz) spectra were recorded on a Varian XR200 spectrometer, using tetramethylsilane as an internal standard. Infrared spectra were recorded on a Perkin Elmer Paragon 1000PC FT-IR spectrophotometer as

Nujol mulls using NaCl windows. Microanalyses were performed by the University of Cape Town Microanalytical Laboratory.

Synthesis of salicylaldimine ligands $\text{HL}^1 - \text{HL}^7$

To a methanol solution (15 mL) of the appropriately substituted 2-hydroxybenzaldehyde (12 mmol) were added formic acid (0.5 mL) and the corresponding aromatic amine (16 mmol). The resulting reaction mixture was stirred at r. t. for approximately 15 h. During this time a solid precipitated from the solution and was isolated by filtration, washed with cold methanol and dried under vacuum. The salicylaldimine ligands were obtained as light yellow to orange yellow solids in yields of 65–93 %.

Synthesis of copper complexes **1–8**

Copper acetate monohydrate (0.5 mmol) and the appropriate Schiff base ligand (1 mmol) were refluxed in methanol (20 mL) for 4 h. During this time a solid precipitated from solution. The reaction mixture was cooled to 0 °C for approximately 15 min and the solid was isolated by vacuum filtration. Complex **8** was prepared using a 1 : 1 mole ratio of ligand and HL^7 to copper acetate. Complexes were recrystallized by slow diffusion of ethanol into concentrated dichloromethane solutions of the complexes.

General procedure for the hydroxylation of phenol

A 12 place RADLEYS Heated Carousel Reaction Station fitted with a reflux unit as well as a gas distribution system was used to perform the hydroxylation reactions. In a typical reaction, phenol (1 mmol) and the appropriate catalyst (0.1 mmol) were placed in a 50 mL glass reaction vessel followed by the appropriately buffered solution which was saturated with oxygen (10 mL). The temperature of the reaction mixture was brought to 110 °C under an oxygen atmosphere and the mixture stirred at this temperature for 15 min. A 6 % H_2O_2 (w/w) solution (1 mmol) was added and the reaction mixture was stirred at 110 °C under an oxygen atmosphere for a further 6 h. The reaction mixture was cooled to r. t. and a 1 mL sample withdrawn, filtered through a syringe filter and diluted 20 times. The consumption of phenol and the oxidation products obtained were analyzed with a HP 1090 Liquid Chromatograph unit equipped with a ZORBAX SB-C18 column of dimension 4.6×150 mm. The mobile phase used was a mixture of 0.1 % formic acid solution and acetonitrile.

X-Ray crystallography

Suitable crystals for X-ray analysis were obtained by slow diffusion of ethanol into dichloromethane solutions of the complexes **2**, **5** and **8**. Crystals of the complexes were mounted on glass capillaries and transferred to a Rigaku R-Axis IIC diffractometer. Diffracted intensities

were measured at ambient temperature, using graphite-monochromated $\text{MoK}\alpha$ radiation ($\lambda = 0.71073 \text{ \AA}$) from a RU-H3R rotating anode operated at 50 kV and 90 mA. Ninety oscillation photographs with a rotation angle of 2° were collected and processed using the CrystalClear software package. Empirical corrections were applied for the effects of absorption using the REQAB program under CrystalClear. The structures were solved by Direct Methods [19] and refined using full-matrix least-squares calculations on F^2 (SHELXL-97) [20] on all reflections, both programs operating under the WinGX program package [21]. Anisotropic thermal displacement parameters were refined for all non-hydrogen atoms; the hydrogen atoms were included as a riding contribution. Structural illustrations have been drawn with ORTEP-3 for Windows [22] under WinGX [21] (Figs. 1, 2 and 3).

Supplementary crystallographic data for this paper have been deposited at The Cambridge Crystallographic Data Centre [23].

Complex 2: A needle-shaped brownish-green crystal with approximate dimensions $0.15 \times 0.15 \times 0.3 \text{ mm}$. Refinement of 206 parameters based on all 3230 reflections yielded $R_1 = 0.055$ and $wR_2 = 0.114$ for $I \geq 2\sigma(I)$ (2307 reflections) and $R_1 = 0.069$ and $wR_2 = 0.119$ for all reflections; maximum and minimum residual electron density: $0.45; -0.86 \text{ e \AA}^{-3}$.

Complex 5: A dark-green crystal fragment with approximate dimensions $0.25 \times 0.25 \times 0.40 \text{ mm}$. Refinement of 151 parameters based on all 2235 reflections yielded $R_1 = 0.032$ and $wR_2 = 0.090$ for $I \geq 2\sigma(I)$ (2129 reflections) and $R_1 = 0.032$ and $wR_2 = 0.091$ for all reflections; maximum and minimum residual electron density: $0.27; -0.35 \text{ e \AA}^{-3}$.

Complex 8: A needle-shaped greyish-green crystal with approximate dimensions $0.15 \times 0.15 \times 0.40 \text{ mm}$. The hydroxyl hydrogen atom on O(5) was located from a difference map and refined with a fixed isotropic thermal parameter $= 0.05 \text{ \AA}^2$. Refinement of 589 parameters based on all 9953 reflections yielded $R_1 = 0.064$ and $wR_2 = 0.147$ for $I \geq 2\sigma(I)$ (7185 reflections) and $R_1 = 0.106$ and $wR_2 = 0.167$ for all reflections; maximum and minimum residual electron density: $1.33; -0.40 \text{ e \AA}^{-3}$.

Acknowledgements

We would like to acknowledge the National Research Foundation and the WRC, South Africa for financial support. This work was also supported by the Swedish Research Council (Natural and Engineering Sciences, VR-NT), by Sida/NRF (Sweden – South Africa Research Partnership Programme, Project SRP-2001-040) and by The Royal Society of Arts and Sciences in Gothenburg (KVVS).

- [1] J. Zhang, Y. Tang, J.-Q. Xie, J.-Z. Li, W. Zeng, C.-W. Hu, *J. Serb. Chem. Soc.* **2005**, *70*, 1137.
- [2] J. Zhang, Y. Tang, J.-Q. Xie, Z.-R. Song, L. Wing, C.-W. Hu, *React. Kinet. Catal. Lett.* **2005**, *85*, 269.
- [3] J. Q. Xie, J.-Z. Li, X.-G. Meng, C.-W. Hu, X.-C. Zeng, *Trans. Met. Chem.* **2004**, *29*, 388.
- [4] H. Liu, G. Lu, T. Guo, Y. Guo, *Appl. Catal. A. Gen.* **2005**, *293*, 153.
- [5] H. Liu, G. Lu, Y. Guo, Y. Guo, J. Wang, *Chem. Eng. J.* **2006**, *116*, 179.
- [6] J. A. Martens, Ph. Buksen, P. A. Jacobs, A. vander Pol, J. H. C. van Hooff, C. Ferrini, H. W. Kouwenhoven, P. J. Kooyman, H. van Bekkum, *Appl. Catal. A. Gen.* **1993**, *99*, 71.
- [7] C. Wang, S. Friedrich, T. R. Youkin, R. T. Li, R. H. Grubbs, D. A. Bansleben, M. W. Day, *Organometallics* **1998**, *17*, 3149.
- [8] R. B. Coles, C. M. Harris, E. Sinn, *Inorg. Chem.* **1969**, *8*, 2607.
- [9] W.-H. Chen, H.-H. Wei, G.-H. Lee, Y. Hung, *Polyhedron* **2001**, *20*, 515.
- [10] E. Schön, D. A. Plattner, P. Chen, *Inorg. Chem.* **2004**, *43*, 3164.
- [11] E. Tas, M. Aslanoglu, M. Ulusoy, H. Temel, *J. Coord. Chem.* **2004**, *57*, 677.
- [12] E. Tas, M. Aslanoglu, M. Guler, M. Ulusoy, *J. Coord. Chem.* **2004**, *57*, 583.
- [13] S. F. Mapolie, J. L. Van Wyk, unpublished results.
- [14] A. Dubey, V. Rives, S. Kannan, *J. Mol. Catal. A* **2002**, *181*, 151.
- [15] Y. H. Hue, A. Gedeon, J. L. Bonardet, N. Melush, J. B. D'Espinoise, J. Fraissard, *Chem. Commun.* **1999**, 1967.
- [16] C. Liu, Y. Shan, X. Yang, X. Ye, Y. Wu, *J. Catal.* **1997**, *168*, 35.
- [17] L. Wang, A. Kong, B. Chen, H. Ding, Y. Shan, M. He, *J. Mol. Catal. A* **2005**, *230*, 143.
- [18] J. N. Parrk, J. Wang, K. Y. Choi, W.-Y. Dong, S.-J. Hong, C. W. Lee, *J. Mol. Catal.* **2006**, *247*, 73.
- [19] SIR92: A. Altomare, G. Cascarano, C. Giacovazzo, A. Guagliardi, *J. Appl. Crystallogr.* **1993**, *26*, 343.
- [20] G. M. Sheldrick, SHELX97 (Release 97-2), Programs for the Determination of Crystal Structures, University of Göttingen, Göttingen (Germany) **1998**.
- [21] L. J. Farrugia, *J. Appl. Crystallogr.* **1999**, *32*, 837.
- [22] L. J. Farrugia, *J. Appl. Crystallogr.* **1997**, *30*, 565.
- [23] CCDC 622393 – 622395 contain the supplementary crystallographic data for this paper. These data can be obtained free of charge from The Cambridge Crystallographic Data Centre via www.ccdc.cam.ac.uk/data_request/cif.